Parameter Identification of a PMSG Using a PSO Algorithm Based on Experimental Tests

A. J. Mahdi, W. H. Tang *Member, IEEE,* Q. H. Wu *Senior Member, IEEE*

***Abstract*— An accurate model for a permanent magnet synchronous generator (PMSG) is important for the design of a high-performance PMSG control system. The performance of such control systems is influenced by PMSG parameter variations under real operation conditions. In this paper, the electrical parameters of a PMSG (the phase resistance, the phase inductance and the rotor permanent magnet (PM) flux linkage) are identified by a particle swarm optimisation (PSO) algorithm based on experimental tests. The advantages of adopting the PSO algorithm in this research include easy implementation, a high computational efficiency and stable convergence characteristics. For PMSG parameter identification, the normalised root mean square error (NRMSE) between the measured and simulated data is calculated and minimised using PSO.**

***Index Terms*— Parameter identification, permanent magnet synchronous generator (PMSG), particle swarm optimisation (PSO), modelling, dSPACE.**

I. INTRODUCTION

Recently, PMSGs have been widely used in variable-speed power generation systems especially in wind turbine generator (WTG) systems [1]. A PMSG has a number of attractive features, such as a high efficiency, a high torque to inertia ratio, a high torque to volume ratio, a high air-gap flux density, a high power factor, high acceleration and deceleration rates, lower maintenance cost and a compact structure [2].

Generally, the performance of a PMSG control system is dependent on the good knowledge of generator parameters that vary with the temperatures and the frequencies [3]. The accuracy of a PMSG model is determined by its parameters, which are the phase resistance, the phase inductance and the PM flux linkage. These parameters should be identified as accurate as possible. There are many analytical methods which have been proposed for calculating parameters of electrical machines [4], [5]. Most of these methods are based on physical specifications of a PMSG such as mechanical dimensions, stator winding specifications and rotor PM characteristics. As most of these information is unknown, these analytical methods are not feasible for calculating optimised parameters. On the other hand, experimental methods for parameter identification, have also been developed such as a dc current decay test [6], a no-load test, a blocked-rotor test and a load test [7]. In the dc current test, the steady-state parameters can be identified without considering transient operating conditions. Implementing the blocked-rotor test gives inaccurate parameters, because the voltages and currents are not measured at normal operating conditions. In the load test, accurate parameters may be identified but this test requires complex experimental procedures. In [8], the electrical parameters of a permanent magnet synchronous motor (PMSM) are identified using an adaptive identification algorithm, which is based on output identification errors. The electrical parameters (the phase resistance, the phase inductance and the iron loss resistance) were identified in steady-state operating conditions, while the mechanical parameters (the electromotive force constant, the inertia and the viscous friction) were identified experimentally in dynamic conditions.

Because the rotor of PMSGs includes PMs and there are no open-circuit and short-circuit states, the influence of PM characteristics must be considered in calculations of PMSG parameters. As a result, the methods based on experimental tests are also not accurate enough identify to parameters of a machine [9]. A PSO is a stochastic optimisation method, which is based on the principles of natural biological evolution [10]. It has been used for optimising parameters of electrical machines and tuning PI controllers [11]. In [12], a new approach based on PSO is demonstrated for parameter identification with a nonlinear PMSM model. The motor stator resistance and the disturbed load torque are identified for variable-frequency drive system applications. In [13], the parameters of a PID controller are optimally tuned by an adaptive particle swarm optimisation (APSO). Although PSO is a robust optimisation algorithm, it generally takes a long time to optimise parameters of a system because of its slow convergence speed [14]. In this paper, the bounds of parameters are minimised using results of experimental tests. The aim of this procedures of the PSO algorithm is to increase the accuracy of parameter identification, reduce the search space of parameters and decrease the convergence time (the time that algorithm spends to find the global optimal solution) of the PSO algorithm.

This paper is organised as follows: a PMSG model is represented in Section II. Parameter measurements of a PMSG are given in Section III. Section IV illustrates the basics of a PSO algorithm. The results and discussion are demonstrated in Section V. Finally in Section VI, a conclusion is given.

II. PMSG MODEL

The operation principles of PMSGs are similar to conventional synchronous generators except that an excitation winding is replaced by permanent magnets [15]. Figure 1

A. J. Mahdi, W. H. Tang and Q. H. Wu are with the Department of Electrical Engineering and Electronics, The University of Liverpool, Liverpool, L69 3GJ, U.K. Corresponding author is W. H. Tang, Tel: +44 151 7944615, Fax: +44 151 7944540, E-mails: ali.mahdi@liv.ac.uk, whtang@liv.ac.uk and qhwu@liv.ac.uk.

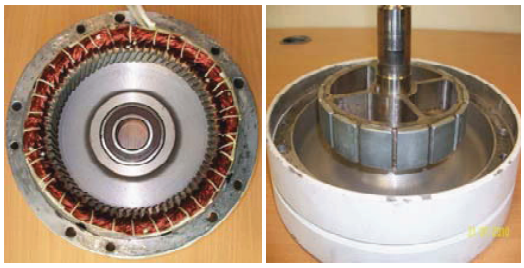

Stator PM rotor

Fig. 1. The stator and the PM rotor of a PMSG.

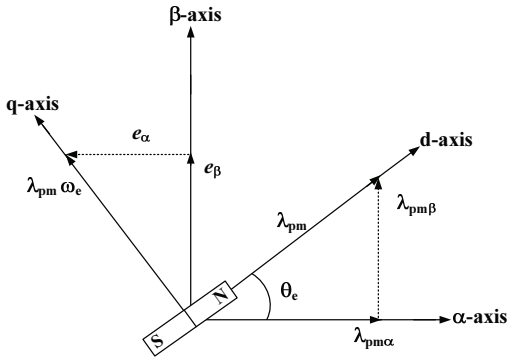

Fig. 2. Phasor diagram of the PM rotor flux linkage and back-emf in the stationary reference frame.

shows the stator and the PM rotor of the PMSG used in this study. Figure 2 shows the phasor diagram of a PMSG in the stator orthogonal coordinate system ($\alpha\beta$-axis). As can be seen from Fig. 2, $\lambda_{\rm pm}$ is the magnitude of the rotor PM flux linkage; $\lambda_{{\rm pm}\alpha}$ and $\lambda_{{\rm pm}\beta}$ are the α-axis and β-axis rotor PM flux linkages; e_α and e_β are the α-axis and β-axis back-emfs; $\omega_{\rm e}$ and $\theta_{\rm e}$ are the electrical angular rotor speed and position respectively; and $\lambda_{\rm pm}\omega_{\rm e}$ is the magnitude of the back-emf.

There are two types of PMSGs which are classified according to the location of PMs on the rotor, i.e. the surface-mounted permanent magnet synchronous generators (SPMSGs) and the interior permanent magnet synchronous generators (IPMSGs). The type of the PMSG used in this study is a SPMSG. The main difference between a SPMSG and an IPMSG is that the later has a saliency on the rotor and the d-axis inductance is larger than the q-axis inductance. This difference between the d-axis and q-axis inductances is due to either the asymmetric structure of the PMSG or the flux induced magnetic saturation due to PM [16].

Because of the complexity modelling of the nonlinearity behavior of a PMSG which comes from the magnetic saturation of the iron core, a simplified PMSG model is sufficiently considered for most control systems [17]. In this research, a PMSG is accurately modelled using a two-axis representation under the assumption that the saturation of the iron core and magnetic losses are neglected. Moreover, symmetrically 3-phase sinusoidal currents are considered and the rotor does not contain damper windings. The instantaneous voltage equations of a PMSG in the $\alpha\beta$-axis can be represented as [18]:

$$v_\alpha = R_{\rm s} i_\alpha + \frac{d\lambda_\alpha}{dt}, \tag{1}$$

$$v_\beta = R_{\rm s} i_\beta + \frac{d\lambda_\beta}{dt}, \tag{2}$$

where v_α and v_β are the α-axis and β-axis stator voltages; i_α and i_β are the α-axis and β-axis stator currents; $R_{\rm s}$ is the phase resistance of the stator winding; λ_α and λ_β are the stator magnetic fluxes which can be expressed (Fig. 2) as follows.

$$\lambda_\alpha = L_\alpha(\theta_{\rm e}) i_\alpha + \lambda_{\rm pm}\cos\theta_{\rm e}, \tag{3}$$

$$\lambda_\beta = L_\beta(\theta_{\rm e}) i_\beta + \lambda_{\rm pm}\sin\theta_{\rm e}, \tag{4}$$

where L_α and L_β are the inductances in the $\alpha\beta$-axis. In a SPMSG, these inductances are equal to the self phase inductance, $L_{\rm s}$, of a stator winding and independent to rotor positions [17].

Substituting λ_α and λ_β of (3), and (4), into (1), and (2), respectively, rearranging and solving the later two equations, the estimated α-axis and β-axis stator currents ($i_{\alpha,\rm est}$ and $i_{\beta,\rm est}$) are obtained as follows.

$$\frac{d}{dt} i_{\alpha,\rm est} = \frac{1}{L_{\rm s}}(v_\alpha - R_{\rm s} i_{\alpha,\rm est} - e_{\alpha,\rm est}), \tag{5}$$

$$\frac{d}{dt} i_{\beta,\rm est} = \frac{1}{L_{\rm s}}(v_\beta - R_{\rm s} i_{\beta,\rm est} - e_{\beta,\rm est}). \tag{6}$$

From Fig. 2, It is seen that the estimated α-axis and β-axis back-emfs ($e_{\alpha,\rm est}$ and $e_{\beta,\rm est}$) depend on the rotor position angle which can be measured by an encoder. In practice, an encoder cannot measure an accurate initial position angle, which may lead to wrong calculations of $e_{\alpha,\rm est}$ and $e_{\beta,\rm est}$ [19]. In this research, an estimator based on an adaptive PI controller is developed for the estimation of $e_{\alpha,\rm est}$ and $e_{\beta,\rm est}$ as follows.

$$e_{\alpha,\rm est} = k_{\rm p,emf}(i_{\alpha,\rm est} - i_{\alpha,\rm m}) + k_{\rm i,emf}\int_0^t (i_{\alpha,\rm est} - i_{\alpha,\rm m})d\tau \tag{7}$$

$$e_{\beta,\rm est} = k_{\rm p,emf}(i_{\beta,\rm est} - i_{\beta,\rm m}) + k_{\rm i,emf}\int_0^t (i_{\beta,\rm est} - i_{\beta,\rm m})d\tau, \tag{8}$$

where $k_{\rm p,emf}$ and $k_{\rm i,emf}$ are the proportional and integral factors of the back-emf estimator; $i_{\alpha,\rm m}$ and $i_{\beta,\rm m}$ are the measured α-axis and β-axis stator currents. However, the proposed back-emf estimator is very easy to implement and includes a few parameters to be tuned using a PSO algorithm.

III. PMSG PARAMETER MEASUREMENTS

In this section, the particular experimental tests for calculating the PMSG parameters are briefly described. The measured parameter values can be utilised for choosing the parameter boundaries of the proposed PSO algorithm. In this research, the PM flux linkage is calculated by a no-load test. While, the phase resistance and inductance are calculated by a load test. In the proposed load test, the only stator winding of a PMSG is connected to a variable-voltage rotary regavolt transformer. The advantage of using a load test is its easy implementation compared with a short-circuit test.

A. PM Flux Linkage

In a no-load test, the PMSG is driven by a 3-phase induction motor at various speeds and the stator winding is open-circuited. The terminal 3-phase voltages and the rotor speed are measured. The back-emf is considered as the open-circuit RMS stator phase voltage, $v_{\rm s}$. The RMS PM flux linkage, $\lambda_{\rm pm}$, is given as [20]:

$$\lambda_{\rm pm} = \frac{v_{\rm ab}}{\omega_e} \times \sqrt{\frac{2}{3}}, \tag{9}$$

where $v_{\rm ab}$ is the open-circuit line-to-line maximum voltage. Figure 3 illustrates the measured PM flux linkage values under frequency variations.

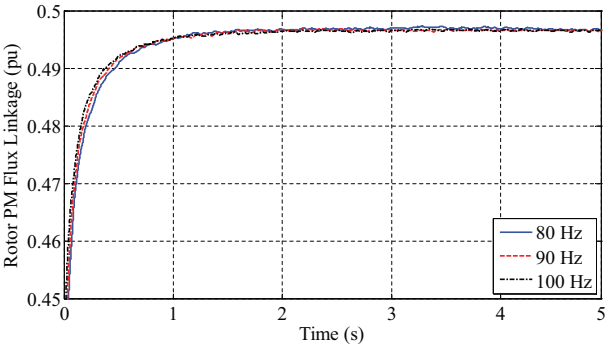

Fig. 3. Experimental PM flux linkage values in a no-load test.

B. Phase Resistance and Phase Inductance

There is a significant variation in the phase resistance of a stator winding over an operating temperature range. Measuring of this variation in resistance gives an estimate the temperature rise of a stator winding. For a 10 °C resolution in the operating temperature range, the resistance must be estimated to about 5 mΩ accuracy [21]. As the stator winding of the PMSG used in this study is connected in a star connection and there is no neutral point supplied, the measured inductance is the inductance between phase A and phase B which is given as:

$$L_{\rm line} = L_{\rm sa} + L_{\rm sb} - L_{\rm mab} - L_{\rm mba}, \tag{10}$$

where $L_{\rm sa}$ and $L_{\rm sb}$ are the self inductances of phase A and phase B respectively and $L_{\rm mab}$ and $L_{\rm mba}$ are the mutual inductance between phase A and phase B respectively. The self and mutual inductances can be expressed as:

$$L_{\rm sa} = L_{\rm ls} + L_{\rm o} - L_{\rm ms}\cos(2\theta_{\rm e}), \tag{11}$$

$$L_{\rm mab} = L_{\rm ba} = -\frac{1}{2}L_{\rm o} - L_{\rm ms}\cos(2\theta_{\rm e} - \frac{2\pi}{3}), \tag{12}$$

where $L_{\rm ls}$ is the leakage inductance of the stator winding due to its leakage flux, $L_{\rm o}$ is the average inductance due to the air-gap flux and $L_{\rm ms}$ is the saliency inductance due to the electrical rotor position $\theta_{\rm e}$. $L_{\rm o}$ and $L_{\rm ms}$ are given as:

$$L_{\rm o} = \frac{1}{2}(L_d + L_q), \tag{13}$$

$$L_{\rm ms} = \frac{1}{2}(L_d - L_q). \tag{14}$$

In addition, $L_{\rm sa}$ and $L_{\rm mab}$ depend on rotor positions, so that the d-axis should be aligned with the a-axis in order to make θ_e equal to zero and consequently the self inductance becomes independent to rotor positions. This condition is only important for a salient rotor machine, IPMSG. In this research, the proposed PMSG is a non-salient type, SPMSG, therefore it is not required to align the d-axis with the a-axis.

As mentioned above that in a SPMSG, the d-axis inductance equals to the q-axis inductance, this consideration makes $L_{\rm ms}$ equals to zero. If $L_{\rm ls}$ is neglected, then $L_{\rm sa}$ is equal to $L_{\rm o}$. In practice, $L_{\rm sa}$ can be measured by several methods such as a short-circuit test, a load test and a blocked-rotor test. In this research, the phase stator resistance and reactance are calculated and demonstrated (Fig. 4) using a load test under a wide range of current variations. The idea of measuring phase resistance and reactance is based on calculating the magnitude of the phase impedance and the phase-shift between the phase voltage and current. It can be seen from Fig. 4 that the phase resistance and reactance of the stator winding increase with current increasing due to the winding temperature changes and magnetic saturation.

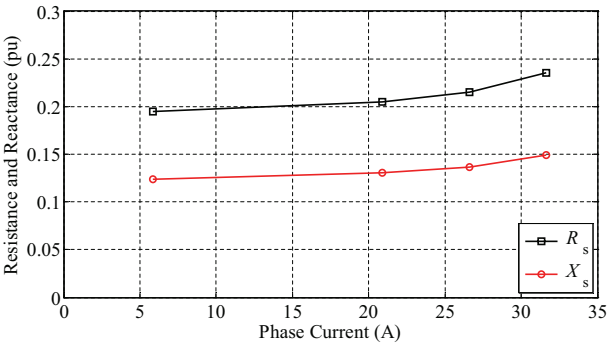

Fig. 4. Experimental stator phase resistance and reactance in a load test.

IV. PSO ALGORITHM

A PSO algorithm is an evolutionary computation method inspired by social behaviors of bird flocking during searching food. Each bird may be called a "particle" in a population, that is a "swarm" moving over a "search space" to achieve an objective. In a PSO algorithm, the position of an particle illustrates the solution of an optimisation problem. Each particle moves in the search space with a velocity according to the previous optimum individual solution and the previous optimum global solution [22].

It uses a population of N particles, which is the dimension of the search space. The state of the ith particle is represented as $x_i(t) = [x_{i1}(t), x_{i2}(t), ..., x_{iN}(t)]$. The previous best state, $pbest$, is written as $p_i(t) = [p_{i1}(t), p_{i2}(t), ..., p_{iN}(t)]$. The index of the best state in the global set, $gbest$, is represented as $p_g(t) = [p_{g1}(t), p_{g2}(t), ..., p_{gN}(t)]$. The moving velocity, $v_i(t)$, is represented as $v_i(t) = [v_{i1}(t), v_{i2}(t), ..., v_{iN}(t)]$.

A PSO algorithm can be implemented using (15), and (16),

[10].

$$v_i(k+1) = \omega v_i(k) + c_1 rand_1(p_i(k) - x_i(k)) + c_2 rand_2(p_g(k) - x_i(k)), \quad (15)$$

$$x_i(k+1) = x_i(k) + v_i(k+1), \quad (16)$$

where k is an iteration number, ω is an inertia weight factor, c_1 and c_2 are constants which represent the control parameters of the PSO algorithm. If c_1 and c_2 are selected as small values, the individual may move far from the objective regions before being tugged back. But if c_1 and c_2 are selected as large values, the individual may move in sudden towards objective regions. Generally, c_1 and c_2 are selected around 2. The parameters $rand_1$ and $rand_2$ are random values, which are uniformly distributed random numbers in [0, 1]. It is important to know that these values are randomly generated and they may change during each iteration [23].

As mentioned previously, the purpose of using the proposed PSO algorithm is to search the optimal parameters of the PMSG model by minimising the normalized root mean square errors (NRMSEs) of the current, $e_{\rm i}$, back-emf, $e_{\rm f}$, and rotor speed, e_ω. Figure 5 illustrates how the PSO algorithm is used with the PMSG model to identify parameters of a real PMSG by measuring the 3-phase voltages, $v_{\rm abc}$, and 3-phase currents, $i_{\rm abc}$. The estimated α-axis and β-axis currents, $i_{\alpha\beta,\rm est}$, the estimated α-axis and β-axis back-emfs, $e_{\alpha\beta,\rm est}$, and the estimated rotor speed, $\omega_{\rm m,est}$, are compared with the measured α-axis and β-axis currents, $i_{\alpha\beta,\rm m}$, the measured α-axis and β-axis back-emfs, $e_{\alpha\beta,\rm m}$, and the measured rotor speed, $\omega_{\rm m,m}$, respectively to calculate NRMSEs. These NRMSEs are then minimised by the proposed PSO algorithm to drive the optimal parameters of the PMSG model. In this research, the rotor speed $\omega_{\rm m}$ and position $\theta_{\rm e}$ are measured for monitoring purpose.

Thus, for each particle of a population in PSO, its total fitness value is given as:

$$F = min(e_{\rm i} + e_{\rm f} + e_\omega), \quad (17)$$

A NRMSE can be calculated (in percent) according to:

$$e = \sqrt{\frac{1}{n}\sum_{i=1}^{n}(A_i - E_i)^2} \times \frac{100}{M}, \quad (18)$$

where A_i and E_i are the actual and estimated values for the PMSG state variables respectively, n is the number of the samples involved for PSO implementation and M is the mean of the estimated value. In the proposed PSO algorithm, each particle contains two parameters which are $k_{p,emf}$ and $k_{i,emf}$. On the other hand, the search space of the PSO has two dimensions and the particles must move in a three dimensional space. As mentioned before that the objective of the proposed PSO is to minimise $e_{\rm f}$, $e_{\rm i}$ and e_ω, thus for each iteration, it is required to calculate these errors from the Simulink model of the PMSG and update their values inside the PSO algorithm. Finally, a maximum number of iterations are generally predefined in order to terminate the PSO algorithm. In this work, the PSO algorithm is terminated when the fitness value of solutions have small changes after multiple iterations in the searching process. On the other hand, the termination is true when $|F_i(x) - F_{i-1}(x)| < \varepsilon$, where ε is a predefined error limit.

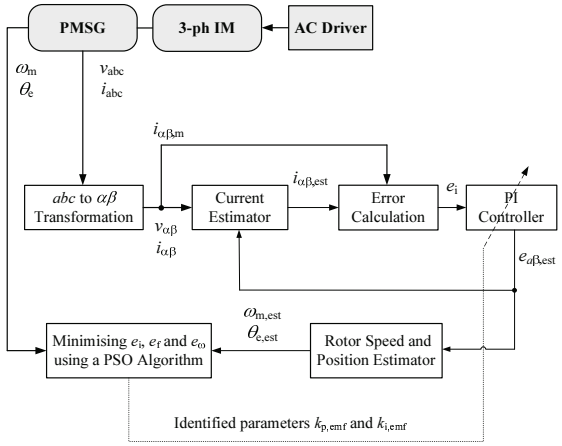

Fig. 5. Scheme of the PMSG parameters identification using a PSO algorithm.

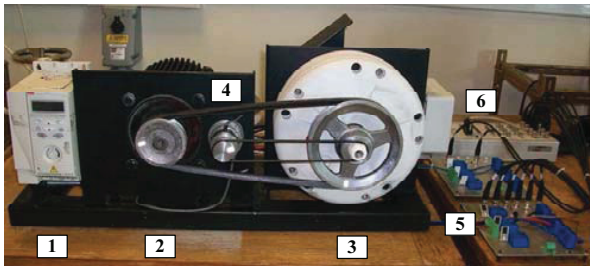

Fig. 6. Parts of the developed test bench: (1) a variable-speed ac driver, (2) a 3-phase induction motor, (3) a PMSG, (4) an encoder, (5) voltage and current sensor boards, (6) a dSPACE controller.

V. RESULTS AND DISCUSSION

The experimental tests have been implemented with an experimental PMSG (type GL-PMG-500A). The test bench is shown in Fig. 6. The proposed test bench consists of a PMSG which is coupled to a 3-phase induction motor (IM) that is controlled by a variable-speed ac driver. The measurements are sampled by a dSPACE DS1104 controller. The test bench is equipped with voltage transducers (type LV25-p), current transducers (type LA55-p) and an encoder to measure the rotor speed and position. It is worth noting that all the components used in the proposed test bench are commercially available.

The parameters of a PMSG model (which includes a back-emf estimator) are optimised (using the proposed PSO) and listed in Table II. It is apparent that, these parameters vary with operating conditions due to the variation of the measured physical parameters.

Table I presents the comparison results of the percentage NRMSEs under three test cases. In case 1, the back-emf is calculated using the measured rotor speed and position. In cases 2 and 3, the back-emf is estimated from a back-emf

TABLE I

PERCENTAGE NRMSES FOR A COMPARISON UNDER ROTOR SPEED VARIATIONS

	Case 1 Using Measured Parameters			Case 2 Using Fixed Parameters			Case 3 Using Optimised Parameters		
Rotor Speed, (rpm)	e_i**(%)**	e_f**(%)**	e_ω**(%)**	e_i**(%)**	e_f**(%)**	e_ω**(%)**	e_i**(%)**	e_f**(%)**	e_ω**(%)**
Low, 75	85.83	4.61	4.76	2.41	6.19	7.11	2.91	4.47	5.07
Rated, 375	31.82	4.26	4.33	0.48	4.85	4.87	0.39	5.74	5.86
High, 750	43.14	5.23	5.36	3.96	5.61	5.73	1.32	6.11	6.23

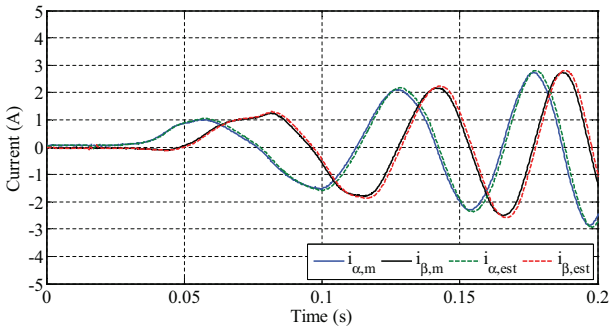

Fig. 7. Experimental and estimated α and β currents in the transient.

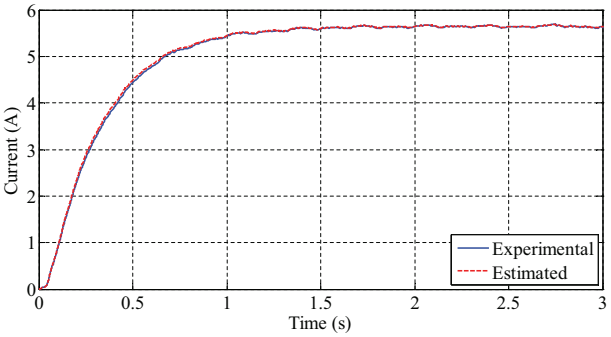

Fig. 8. Experimental and estimated phase currents.

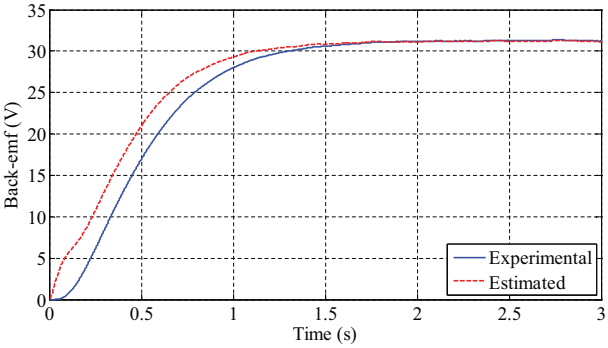

Fig. 9. Experimental and estimated back-emfs.

TABLE II

OPTIMAL PARAMETER VALUES OF THE PMSG MODEL USING THE PROPOSED PSO ALGORITHM

Rotor Speed, (rpm)	R_s **(pu)**	X_s **(pu)**	$k_{p,emf}$	$k_{i,emf}$
Low, 75	0.018	0.046	66.39	29.32
Rated, 375	0.027	0.346	54.48	39.08
High, 750	0.033	0.842	125.58	26.90
Fixed parameter	0.026	0.334	82.15	31.77

estimator. The main difference between case 2 and case 3 is that in case 2, the PI parameters of a back-emf estimator are considered fixed values, while in case 3, the PI parameters are optimally varied with operating conditions. It is seen that, e_i of case 1 are very high (especially at a low speed) because of neglecting the influence of the initial rotor position. In cases 2 and 3, the NRMSEs are significantly reduced because of considering the influence of the initial rotor position in the estimated back-emf. It is clear that the maximal NRMSE in case 1 is 85.83%. While in cases 2 and 3, the maximal NRMSEs are reduced to 7.11% and 6.23% respectively. These results show the effectiveness of the proposed PSO algorithm for parameter identification of the PMSG compared with the numerical methods that mentioned previously.

Figure 7 shows a comparison between the $\alpha\beta$-axis measured and the estimated phase currents in the transient using the optimised parameters. Figure 8 illustrates the magnitude of the measured and estimated phase current. It is seen that, the estimated currents using the accurate PMSG model (with using the optimised parameters) is very close to the measured currents. Figure 9 shows the magnitude of the measured and estimated back-emfs at the rated speed. It is seen that the transient response of a back-emf estimator has an effective time-constant of about 1.5 s.

To further validate the PMSG model, a comparison between the measured rotor speed and position with the estimated rotor speed and position are demonstrated in Figures 10 and 11. It is seen that the estimated rotor speed is very close to the measured rotor speed especially during steady-state operation. Finally, it is worth to note that in this paper, the performance of a PMSG model is improved by minimising the NRMSE (which represents the overall error performance) while in [12], the steady-state error has been considered for measuring the

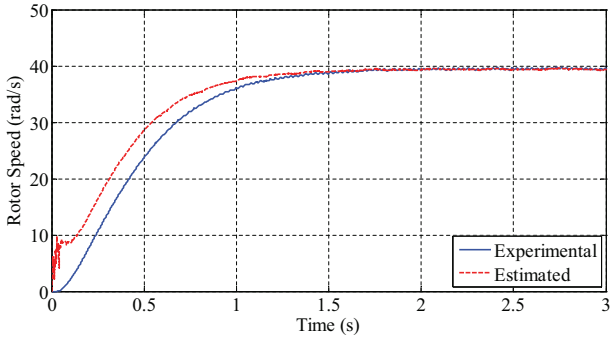

Fig. 10. Experimental and estimated rotor speed.

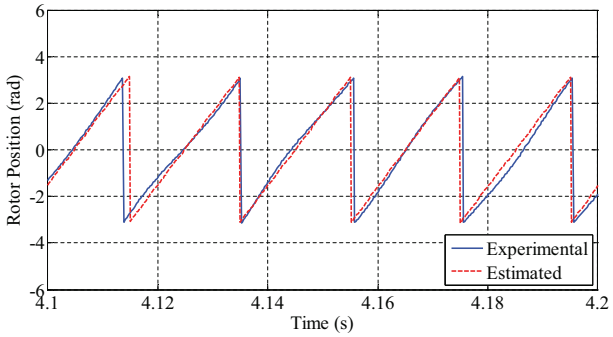

Fig. 11. Experimental and estimated electrical rotor position.

performance of a PSO-based parameter identifier. In addition, in [12] the maximum steady-state speed error is around 1.8 rad/s while in this work, the corresponding error is minimised to 0.25 rad/s (at rated rotor speed) by using the optimised parameters.

VI. CONCLUSION

A PSO algorithm based parameter identification of a PMSG model has been implemented and tested with experimental data. The proposed PSO algorithm used in this research allows results to be obtained with a good accuracy. A close agreement between the experimental measured data and the corresponding simulated data is obtained, which verifies the effectiveness of the proposed PSO algorithm for parameter identification. Further work will be focused on identifications of mechanical parameters of a PMSG.

ACKNOWLEDGMENT

The authors thank Miss. Nicola Telfer who is with the Department of Electrical Engineering and Electronics, The University of Liverpool, for her help during the construction of the mechanical parts of the test bench.

REFERENCES

[1] L.H. Hansen, P.H. Madsen, F. Blaabjerg, H.C. Christensen, U. Lindhard, and K. Eskildsen, "Generators and power electronics technology for wind turbines," *IECON*, vol.3, pp: 2000-2005, 2001.

[2] R. Mittal, K.S. Sandu, and D.K. Jain, "Isolated Operation of Variable Speed Driven PMSG for Wind Energy Conversion System," *IACSIT International Journal of Engineering and Technology*, vol. 1, no. 3, 2009.

[3] C.A. Martins and A.S. Carvalho, "Technological trends in induction motor electrical drives," *Power Tech Proceedings, IEEE Porto*, vol. 2, 2001.

[4] S. Weisgerber, A. Proca, and A. Keyhani, "Estimation of permanent magnet motor parameters," *in Proc. IEEE Ind. Appl. Soc. Annu. Meeting, New Orleans, LA*, pp. 2934, 1997.

[5] K.M. Rahman and S. Hiti, "Identification of machine parameters of a synchronous motor", *Industry Applications Conference, 2003. 38th IAS Annual Meeting. Conference*, vol. 1, pp. 409-415,2003.

[6] S. yamamoto Ara, T., S. Oda, and K. Matsuse, "Prediction of Starting Performance of PM DC Decay Testing Method," *IEEE trans. On industry applications*, vol. 36, pp. 1053-1060, 2000.

[7] B. Stumberger, b.kreca, and B. Hribernik, "Determination of Parameters of Synchronous Motor with Permanent Magnets from Measurement of Load Conditions," *Electric Machines and Drives Conference Record*, pp. WB2/1.1-WB2/1.3, 1997.

[8] T. Senjyu, K. Kinjo, N. Urasaki, and K. Uezato, "Parameter measurement for PMSM using adaptive identification," *Industrial Electronics, Proceedings of the IEEE International Symposium*, vol.3, pp. 711-716, 2002.

[9] X. Zhang, W. Li, W. Chen, D. Xia, and J. Cao, "Numerical analysis for performances of line-start PMSM with solid rotor," *Automation Congress, 2008. WAC 2008. World*, pp. 1-5, 2008.

[10] J. Kennedy and R. C. Eberhart, "Particle swarm optimization," *in Proc. of IEEE International Conference on Neural Networks, Piscataway, NJ, USA*, vol. 4, pp. 1942-1948, 1995.

[11] Z. Lee, "Gaing A particle swarm optimization approach for optimum design of PID controller in AVR system," *Energy Conversion, IEEE Transactions*, vol. 19, pp. 384-391, 2004.

[12] L. Liu, W. Liu, and D.A. Cartes, "Particle swarm optimization-based parameter identification applied to permanent magnet synchronous motors," *Engineering Applications of Artificial Intelligence*, vol. 21, pp. 10921100, 2008.

[13] M. Sridhar, K. Vaisakh, and K. Murthy, "Adaptive PSO Based Tuning of PID- Fuzzy and SVC-PI Controllers for Dynamic Stability Enhancement: A Comparative Analysis," *Emerging Trends in Engineering and Technology (ICETET), 2009 2nd International Conference*, pp. 985-990, 2009.

[14] H. Wei and H. Jingtao, "A New BP Network Based on Improved PSO Algorithm and Its Application on Fault Diagnosis of Gas Turbine," *Lecture Notes in Computer Science*, vol. 4493/2007, pp. 277-283, 2007.

[15] P.C. Krause, O. wasynczuk, and S.D. Sudhoff, Analysis of Electric Machinery, *John Wiley & Sons*, 1995.

[16] G. Elmurr, G., D. Giaouris, J.W. Finch, "Universal PLL Strategy for Sensorless Speed and Position Estimation of PMSM," *IEEE Region 10 and the Third international Conference*, pp. 1-6, 2008.

[17] S. Ostlund and M. Brokemper,"Sensorless Rotor-Position Detection from Zero to Rated Speed for an Integrated PM Synchronous Motor Drive," *IEEE Transactions On Industry Applications*, vol. 32, no. 5, pp. 1158-1165, 1996.

[18] Y. Kung, M. Wang, and C. Huang, "DSP-based adaptive fuzzy control for a sensorless PMSM drive," *IEEE on Control and Decision Conference*, pp. 2379-2384, 2009.

[19] S. Shinnaka and T. Kumakura, "A New Initial-Rotor-Position Estimation Method for SPM Synchronous Motors Using Spatially Rotating High-Frequency Voltage: A Dynamic Simulator Approach Taking Flux Saturation Phenomena into Account," *Electrical Engineering in Japan*, vol. 124, no. 11, pp. 1094-1103, 2004.

[20] N. Mohan, Advanced electric drives: analysis, control and modeling using Simulink, *Minneapolis : MNPERE*, 2001.

[21] S.D. Wilson, P. Stewart, B.P. Taylor, "Methods of Resistance Estimation in Permanent Magnet Synchronous Motors for Real-Time Thermal Management," *IEEE Transactions on Electr. Machines & Drives Res. Group*, vol. 25, no. 3, pp. 698-707, 2010.

[22] Y. del Valle, G. K. Venayagamoorthy, S. Mohagheghi, J.-C. Hernandez, and R. G. Harley, "Particle swarm optimization: basic concepts, variants and applications in power systems," *IEEE Transactions on Evolutionary Computation*, vol. 12, no. 2, pp. 171195, 2008.

[23] P. Umapathy,C. Venkataseshaiah, and M. Arumugam, "Particle Swarm Optimization with Various Inertia Weight Variants for Optimal Power Flow Solution Prabha Umapathy," *Hindawi Publishing Corporation Discrete Dynamics in Nature and Society*, 2010.